Catalysis in Human Hypoxanthine-Guanine Phosphoribosyltransferase: Asp 137 Acts as a General Acid/Base†

Yiming Xu‡ and Charles Grubmeyer*

Department of Biochemistry and Fels Institute for Cancer Research and Molecular Biology, Temple University School of Medicine, 3307 North Broad Street, Philadelphia, Pennsylvania 19140

Received October 10, 1997; Revised Manuscript Received December 11, 1997

ABSTRACT: Hypoxanthine-guanine phosphoribosyltransferase (HGPRTase) catalyzes the reversible formation of IMP and GMP from their respective bases hypoxanthine (Hx) and guanine (Gua) and the phosphoribosyl donor 5-phosphoribosyl-1-pyrophosphate (PRPP). The net formation and cleavage of the nucleosidic bond requires removal/addition of a proton at the purine moiety, allowing enzymic catalysis to reduce the energy barrier associated with the reaction. The pH profile of k_{cat} for IMP pyrophosphorolysis revealed an essential acidic group with pK_a of 7.9 whereas those for IMP or GMP formation indicated involvement of essential basic groups. Based on the crystal structure of human HGPRTase, protonation/deprotonation is likely to occur at N7 of the purine ring, and Lys 165 or Asp 137 are each candidates for the general base/acid. We have constructed, purified, and kinetically characterized two mutant HGPRTases to test this hypothesis. D137N displayed an 18-fold decrease in k_{cat} for nucleotide formation with Hx as substrate, a 275-fold decrease in k_{cat} with Gua, and a 500-fold decrease in k_{cat} for IMP pyrophosphorolysis. D137N also showed lower K_D values for nucleotides and PRPP. The pH profiles of k_{cat} for D137N were severely altered. In contrast to D137N, the k_{cat} for K165Q was decreased only 2-fold in the forward reaction and was slightly increased in the reverse reaction. The K_m and K_D values showed that K165Q interacts with substrates more weakly than does the wild-type enzyme. Pre-steady-state experiments with K165Q indicated that the phosphoribosyl transfer step was fast in the forward reaction, as observed with the wild type. In contrast, D137N showed slower phosphoribosyl transfer chemistry, although guanine (3000-fold reduction) was affected much more than hypoxanthine (32-fold reduction). In conclusion, Asp137 acts as a general catalytic acid/base for HGPRTase and Lys165 makes ground-state interactions with substrates.

Hypoxanthine-guanine phosphoribosyltransferase[1] (HGPRTase, EC 2.4.2.8) catalyzes phosphoribosyl transfer from α-D-5-phosphoribosyl-1-pyrophosphate to bases hypoxanthine (Hx) or guanine (Gua) to form the nucleotide IMP or GMP (Scheme 1). The enzyme is important for human health; complete lack of HGPRTase activity in humans causes the Lesch−Nyhan syndrome (*1*), characterized by hyperuricemia, and neural disorders including mental retardation and compulsive self-mutilation behavior (*2*, *3*), whereas partial deficiency of HGPRTase leads to gouty arthritis (*4*). HGPRTase has been proposed as a target for antiparasitic chemotherapy (*5*−*7*), since many pathogenic parasites synthesize purine nucleotides only through salvage pathways.

The crystal structures of human HGPRTase complexes reveal that both GMP and IMP bind to the same active site pocket with minor local alteration in their interactions with enzymic residues (*8*, *9*). In these nucleotide complexes, the ribose 5-phosphate moiety appears to block access of the base moiety to solvent. However, substrates bind in a functionally ordered fashion with PRPP binding first in the forward reaction (IMP or GMP formation) and IMP or GMP first in the reverse reaction (IMP or GMP pyrophosphorolysis; ref *9*). The ordered association of substrates, and the crystal structure, have led us to propose that protein movements induced by PRPP binding might facilitate Hx or Gua access to the active site (*9*). At pH 7.4, phosphoribosyl transfer chemistry occurs rapidly ($k_{forward}$ = 131 s^{-1} and $k_{reverse}$ = 9 s^{-1}) relative to overall catalysis ($k_{cat(forward)}$ = 6.0 s^{-1} and $k_{cat(reverse)}$ = 0.17 s^{-1}). The release of products in both forward and reverse reactions is partially random and largely rate-determining, indicating that protein conformational changes may constitute the rate-limiting steps.

Interactions between the substrates and the enzyme that are responsible for the rapid phosphoribosyl transfer step are unclear, but acid/base catalysis at the purine ring could provide substantial assistence. The pK_a of the imidazole ring proton decreases from 12 for the base to about 1 for the nucleotide (*10*). In solution, Hx exists as a mixture of

† This work was supported by National Institutes of Health Grant GM-52125.

* To whom correspondence should be addressed.

‡ Current address: Department of Biochemistry, Albert Einstein College of Medicine, Bronx, NY 10461.

[1] Abbreviations: AMP−PCP, adenylylmethylenediphosphonate; DTT, dithiothreitol; HGPRTase, hypoxanthine-guanine phosphoribosyltransferase; Hx, hypoxanthine; MES, 2-(*N*-morpholino)ethanesulfonic acid; OPRTase, orotate phosphoribosyltransferase; PCP, methylenebisphosphonate; PCR, polymerase chain reaction; PNP, imidodiphosphate; PRPCP, α-D-5-phosphoribosyl-1-methylenebiphosphonate; PRPNP, α-D-5-phosphoribosyl-1-imidodiphosphate; PRPP, α-D-5-phosphoribosyl-1-pyrophosphate; QAPRTase, quinolinic acid phosphoribosyltransferase; WT, wild-type HGPRTase; XO, xanthine oxidase.

S0006-2960(97)02519-1 CCC: $15.00
Published on Web 03/03/1998

Scheme 1: HGPRTase Reactions

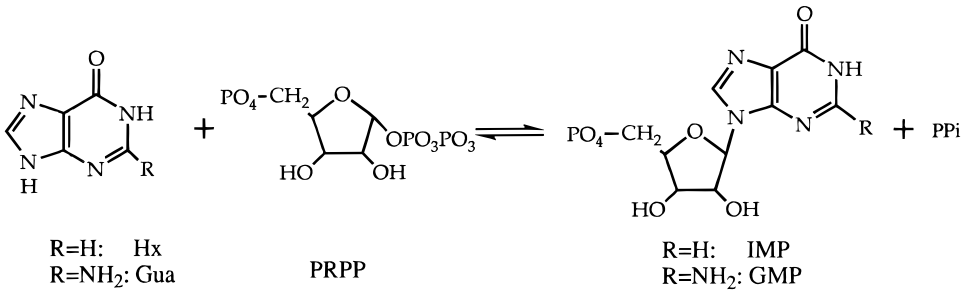

approximately equal amounts of N7 and N9 protonated tautomers (*11*). The crystal structure of HGPRTase indicates that enzymatic proton transfer at N7 is more feasible than at N9, since no enzyme residues were found within hydrogen bond distance of N9 in bound GMP and the phosphoribosyl group would present steric hindrance for N9 protonation and deprotonation (*8*). Studies on the solvolysis of guanosine and adenosine under acidic conditions suggested that protonation at N7 precedes the rate-limiting breakage of N−C bond (*12*, *13*). Among enzymatic reactions, nucleosidic bond cleavage by inosine-uridine nucleoside hydrolase was proposed to follow N7 protonation of leaving hypoxanthine (*14*) and a histidine residue was proposed to act as the general acid (*15*, *16*). Protonation at N7 was also proposed prior to the development of transition states for AMP nucleosidase (*17*) and purine nucleoside phosphorylase (*18*).

The crystal structure of an HGPRTase·GMP complex (*8*) indicates candidate residues for acid/base catalysis. First, Lys 165 and Asp 137 are each within hydrogen bond distance of N7 (the ϵN of Lys 165 and a carboxyl oxygen of Asp 137 are 3.6 and 3.5 Å from N7, repectively), and either could act as the proposed base. Second, the ϵN of Lys 165 is 3.6 Å from the carboxyl oxygen of Asp 137, making it possible that both residues contribute, as a cooperative unit, to acid/base catalysis. Finally, the 5′-phosphate of bound nucleotide is 3.6 Å from a carboxyl oxygen of Asp 137 and could be involved in a proton relay system. We have constructed K165Q and D137N mutant HGPRTases to test these hypotheses. The enzymes were characterized by steady-state and transient kinetics, ligand-binding and pH dependence studies. The results demonstrate that Asp 137 is the catalytic acid/base and Lys 165 is critical for binding of purine moiety, consistent with its location adjacent to O6.

MATERIALS AND METHODS

Materials. [8-^{3}H]Hypoxanthine and [8-^{14}C]guanine were obtained from Moravek Biochemicals, Inc., Brea, CA. DTT was from U. S. Biochemicals. Xanthine oxidase, PRPP, and other biochemicals were from Sigma Chemical Co. Preparation of [β-^{32}P]PRPP was as described (*9*). PRPCP was similarly prepared and purified using AMP−PCP and ribose 5-phosphate.

Construction of K165Q and D137N. Overlapping PCR (*19*) was employed to mutate Lys 165 and Asp 137 individually to glutamine and asparagine, respectively. The mutagenic primers used (Table 1) were purchased from Ransom Hill Bioscience, Inc., Ramona, CA. Plasmid pHPT31 (ref *20*; American Type Culture Collection) was used as the starting template for overlapping PCR using AmpliTaq DNA polymerase (Perkin-Elmer). The final full-length DNA fragments containing the entire coding sequence for HGPRTase were resolved by electrophoresis on low-melting agarose (Gibco BRL Life Technologies, Inc) and digested with restriction enzymes *Nde*I and *Msc*I followed by ligation of the *NdeI*−*MscI* fragment to pET22b(+) (Novagen) previously cut with *Msc*I and *Nde*I. The *hprt* coding region of the recombinant plasmids was sequenced to ensure there were no secondary mutations, and the plasmids were used to transform *Escherichia coli* strain BL21(DE3) for overexpression of the proteins.

Table 1: Mutagenic Primers

mutation	primers[a]
K165Q	5′ GCTTGCTGGTG*CAA*AGGACCCCACG 3′ 3′ CGAACGACCAC*GTT*TCCTGGGGTGC 5′
D137N	5′ GATATAATT*AAC*ACTGGCAAAAC 3′ 3′ CTATATTAA*TTG*TGACCGTTTTG 5′

[a] The italicized codon in each primer specifies the site of mutation.

Enzyme Isolation. The wild-type and mutant HGPRTases were expressed and purified as described previously for the wild-type enzyme (*8*) with the exception that bacterial cultures expressing the mutant protein were induced with 0.05% lactose and 0.5% glycerol at low temperature (22−25 °C; ref *21*) to minimize the formation of inclusion bodies seen with induction by IPTG. The enzymes were homogeneous as judged by SDS−PAGE. Protein was quantified spectrophotometrically using E_{280}(1 mg/mL) = 1.0 (*9*). Subunit molarity was calculated on the basis of M_r = 24 470, calculated from the deduced protein sequence (*22*). The enzyme concentrations reported in this paper refer to the subunit concentration.

Standard Assays. Reaction conditions were as described (*9*). The program HYPER (*23*) was used to evaluate K_m and k_{cat} values which are reported ± standard errors.

pH Profile of HGPRTase. A mixed buffer consisting of 30 mM MES, 30 mM Tris, 30 mM glycine, and 12 mM $MgCl_2$, pH-adjusted with either 1 N HCl or 1 N NaOH, was employed to study the pH dependence of K_m and k_{cat} for the HGPRTases using spectrophotometric assays at 23 °C. The base/nucleotide extinction coefficients used for both forward and reverse reactions were corrected (<10%) for various pH values as necessary. It was experimentally determined that concentrations of the second substrate employed were saturating at all pH values for the three enzymes when K_m values were measured for the other substrate. Under standard assay conditions, all three enzymes gave essentially the same activities in the mixed buffer at pH 7.4 as in 100 mM Tris-HCl and 12 mM $MgCl_2$ at the same pH. The enzymes were stable during the reactions in the range of pH used in this

study. The program HYPER (*23*) was used to determine K_m and k_{cat} at various pH values, and pH profiles were fitted with the programs HBBELL, BELL, or WAVL (*23*) or to rate equations described herein.

Rapid Quenching Experiments. Pre-steady-state kinetic experiments were performed as described (*9*). Base (Hx or Gua) and nucleotide (IMP or GMP) products were separated isocratically with 1% acetonitrile in H_2O on a Waters μBondapak C_{18} column (3.9 × 300 mm). Pre-steady-state product formation was fit to eq 1 (*24*) as described previously

$$[\text{mol product/mol total subunits}] = n(1 - e^{-k_{obs}t}) + k_{cat}t \quad (1)$$

(*9*), where k_{obs} is the first-order rate constant for the rapid phase and n represents the magnitude of the burst of product when the steady-state phase is extrapolated to zero time.

Equilibrium Gel Filtration. The experimental procedures were as previously reported (*9*). To measure the binding of nucleotides to K165Q and D137N, competitive displacement was used. Briefly, binding of [β-^{32}P]PRPP at fixed concentrations was measured using equilibrium gel filtration in the presence of various amounts of nucleotides. The ratio (B) of mol of [β-^{32}P]PRPP bound/mol of total subunits at a given concentration of nucleotide was calculated and the reciprocal of B was plotted versus nucleotide concentration. The plot was fitted to eq 2, which describes the inhibition of ligand

$$\frac{1}{B} = \frac{K_{D(PRPP)} + [PRPP]}{n[PRPP]} + \frac{K_{D(PRPP)}[IMP]}{n[PRPP]K_{D(nucleotide)}} \quad (2)$$

binding by a competitive inhibitor, and in which n is the number of binding sites per subunit. K_D for the nucleotides was estimated from the x-axis intercept of the plot as described by Segel (*25*).

RESULTS

pH-Dependence of WT. Values of k_{cat}, $k_{cat}/K_{m(PRPP)}$, and $k_{cat}/K_{m(PPi)}$ for IMP formation and IMP pyrophosphorolysis and k_{cat} values for GMP formation were determined with WT at pH values from 5.0 to 9.5. For pyrophosphorolysis of IMP, a plot of log k_{cat} versus pH revealed a single essential acidic group with pK_a = 7.88 ± 0.06 (Figure 1A). For nucleotide formation, log k_{cat} versus pH plots with both Gua and Hx (Figure 1B) demonstrated an essential basic group with pK_a between 6 and 7 but showed "hollows" (*26*), possibly arising from slow protonic equilibria. More details with regard to the fits in Figure 1B are given in the Discussion. Plots of log k_{cat}/K_m versus pH for nucleotide formation (Figure 2) implicated one acidic (pK_a = 8.8 ± 0.2) and one basic group (pK_a = 7.1 ± 0.2) in the productive binding of PRPP. For IMP pyrophosphorolysis, the results indicated that two basic groups and one acidic group were required for the productive binding of PPi (data not shown).

Properties and Steady-State Kinetic Parameters of K165Q and D137N. The mutant enzymes were readily purified to homogeneity. K165Q and D137N were both stable proteins and retained 93 and 88% activity, respectively, after 3 h of incubation at 60 °C, comparable to the behavior of WT (91% active). Results from gel filtration of WT, K165Q, and D137N (Superdex 200, Hiload 16/60, Pharmacia) demonstrated that all three enzymes exist as tetramers in 100 mM Tris-HCl, 12 mM $MgCl_2$, 1 mM DTT, pH 7.4, as reported previously for the enzyme purified from human erythrocytes (*27*). Values for K_m, k_{cat}, and k_{cat}/K_m for both K165Q and D137N were measured under standard assay conditions at 23 °C and are presented in Tables 2 and 3. D137N displayed a marked decrease of k_{cat}. In nucleotide formation reactions, a 290-fold decrease was observed with Gua as substrate and an 18-fold decrease with Hx. For pyrophosphorolysis of IMP, a 500-fold reduction was seen. Most K_m values were

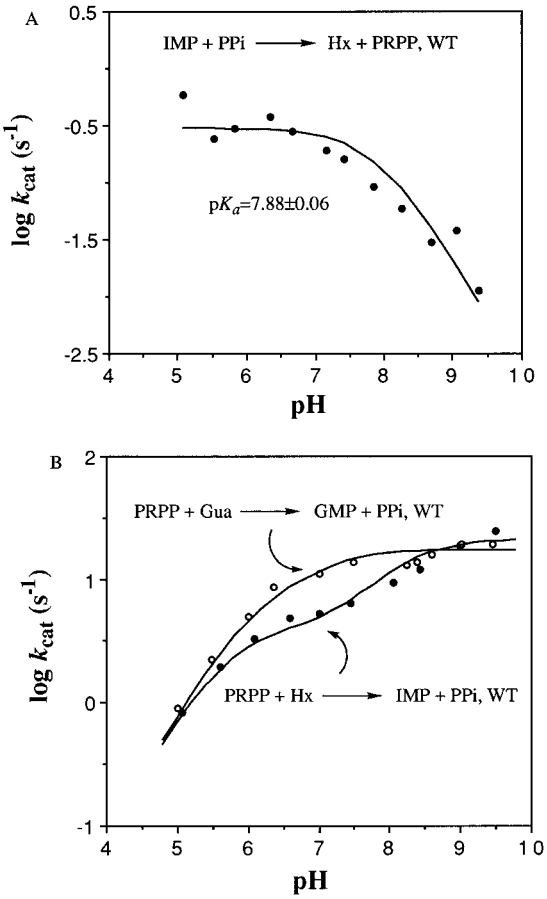

FIGURE 1: pH profiles of k_{cat} for IMP pyrophosphorolysis (A) and nucleotide formation (B) for WT. The line in (A) was generated using HBBELL (*23*). The solid lines in (B) were generated according to Scheme 3 (see Discussion) for IMP (closed circles) and GMP (open circles) formation.

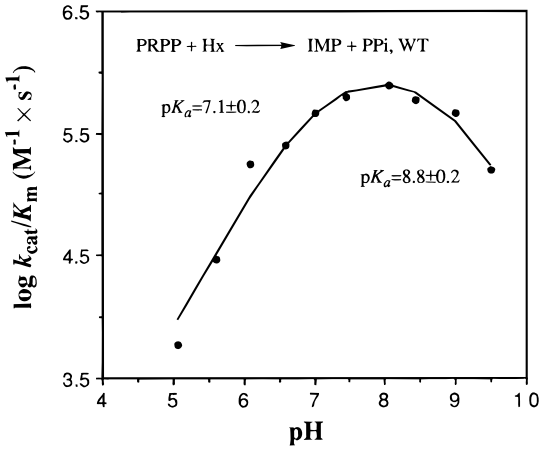

FIGURE 2: pH profile of $k_{cat}/K_{m(PRPP)}$ for WT. The line was generated using BELL (*23*).

Table 2: Kinetic Parameters for Nucleotide Formation

HPRT Reaction								
	PRPP as substrate					PRPCP as substrate		
		K_m (μM)		k_{cat}/K_m (μM^{-1} s^{-1})			PRPCP	
enzyme	k_{cat} (s^{-1})	Hx	PRPP	Hx	PRPP	k_{cat} (s^{-1})	K_m (μM)	k_{cat}/K_m (μM^{-1} s^{-1})
WT	5.9 ± 0.4	0.45 ± 0.14[a]	30.6 ± 2.9	13	0.19	1.08 ± 0.06	5.4 ± 1.4	0.2
K165Q	2.1 ± 0.2	13.6 ± 2.5	30.9 ± 3.1	0.15	0.068	0.55 ± 0.09	37 ± 13	0.015
D137N	0.32	8.5 ± 1.7	4.8 ± 2.0	0.038	0.067	0.093	nd[b]	nd
GPRT Reaction								
	PRPP as substrate					PRPCP as substrate		
		K_m (μM)		k_{cat}/K_m (μM^{-1} s^{-1})			PRPCP	
enzyme	k_{cat} (s^{-1})	Gua	PRPP	Gua	PRPP	k_{cat} (s^{-1})	K_m (μM)	k_{cat}/K_m (μM^{-1} s^{-1})
WT	11.0 ± 0.4	<1	63 ± 6.4	>11.0	0.17	0.91 ± 0.04	5.4 ± 1.0	0.17
K165Q	4.9 ± 0.1	18.5 ± 2.4	70 ± 10	0.26	0.070	0.28 ± 0.04	21 ± 5	0.013
D137N	0.04	0.62 ± 0.35	<1	0.065	>0.04	7.7×10^{-4}	nd	nd

[a] K_m for Hx with WT was measured using radiolabel transfer assays (*9*). [b] nd, not determined.

Table 3: Kinetic Parameters for IMP Pyrophosphorolysis

PPi as Substrate					
		K_m (μM)		k_{cat}/K_m (μM^{-1} s^{-1})	
enzyme	k_{cat} (s^{-1})	IMP	PPi	IMP	PPi
WT	0.15 ± 0.05	4.0 ± 2.7	13.7 ± 3.1	0.038	0.011
K165Q	0.194 ± 0.006	102 ± 29	63 ± 6.3	0.0019	0.0031
D137N	$3.0 \pm 0.1 \times 10^{-4}$	<5	2.5 ± 1.6	$>6 \times 10^{-5}$	1.2×10^{-4}
PNP as substrate					
		K_m (μM)		k_{cat}/K_m (μM^{-1} s^{-1})	
enzyme	k_{cat} (s^{-1})	IMP	PNP	IMP	PNP
WT	0.040 ± 0.002	14.5 ± 1.7	5.9 ± 1.8	2.8×10^{-3}	6.8×10^{-3}
K165Q	0.14 ± 0.03	667 ± 137	229 ± 108	2.1×10^{-4}	1.0×10^{-4}
D137N	1.4×10^{-3}	<10	<10	$>1.4 \times 10^{-4}$	$>1.4 \times 10^{-4}$
PCP as substrate					
		K_m (μM)		k_{cat}/K_m (μM^{-1} s^{-1})	
enzyme	k_{cat} (s^{-1})	IMP	PCP	IMP	PCP
WT	0.12	23 ± 1.8	31 ± 13	5.2×10^{-3}	3.9×10^{-3}
K165Q	0.28 ± 0.08	nd[a]	637 ± 319	nd	4.4×10^{-4}
D137N	1.6×10^{-3}	<10	<10	$>1.6 \times 10^{-4}$	$>1.6 \times 10^{-4}$

[a] nd, not determined because of precipitation of MgPCP.

slightly decreased compared to WT. A 345-fold reduction in k_{cat}/K_m for Hx was observed whereas less profound decreases of k_{cat}/K_m were seen with other substrates. When IMP formation catalyzed by D137N was measured using 10 or 50 mM Tris-HCl or 20 mM NaPi to replace 100 mM Tris-Cl in the standard assay with the ionic strength maintained constant with NaCl, less than 10% change of rates was observed (data not shown).

In contrast to D137N, K165Q showed little change in k_{cat} (2−3-fold decreases for nucleotide formation and a slight increase in the pyrophosphorolysis reaction). However, K_m values for Hx, Gua, and IMP were each increased by 20−30-fold whereas that for PPi was increased by 5-fold and that for PRPP was unchanged. Similarly, k_{cat}/K_m values for Hx, Gua, and IMP were each decreased by 20−80-fold, compared to 2−3-fold decreases for PRPP and PPi.

The methylenebisphophonate and imidodiphosphate analogues of PRPP and PPi have been reported to be substrates for PRTases (*28*, *29*). When PRPCP was used as an alternative for PRPP in the forward reactions (Table 2) for the WT HGPRTase, the k_{cat} values were 6−12-fold reduced compared to those with PRPP. In addition, WT displayed identical k_{cat} values for IMP and GMP formation when PRPCP was the cosubstrate. We have previously shown that the rate of nucleotide release from its binary complex with enzyme (which varies with the nucleotide but would be unchanged with PRPCP compared to PRPP) is the rate-limiting step when PRPP is used and is responsible for the 1.9-fold higher k_{cat} for GMP than IMP formation (*9*). The near equality of k_{cat} with Hx and Gua when PRPCP was utilized indicated that a new rate-limiting step is introduced. The $K_{m(PRPCP)}$ values were the same for both Hx and Gua as the cosubstrate, consistent with the kinetic mechanism (*9*) in which PRPP or PRPCP binds first in the forward reactions, resulting in $K_m = k_{cat}/k_{on}$ for either compound (*30*). Compared to WT, D137N displayed a 1000-fold decrease in k_{cat} with Gua and an 11-fold decrease with Hx when PRPCP was used as an alternative for PRPP (Table 2), the same pattern noted with PRPP. The low activity of D137N with PRPCP prevented precise determination of K_m. K165Q

showed 3−4-fold decreases in k_{cat} with 5−7-fold increases in K_m values (Table 2).

PCP (methylenebisphosphonate) and PNP (imidodiphosphate) were used to replace PPi in the reverse reaction. WT displayed 4-fold decrease in k_{cat} for PNP compared to that for PPi whereas k_{cat} remained the same for PCP as for PPi (Table 3). Values of $K_{m(IMP)}$ were increased by 4−5-fold with PCP or PNP as cosubstrates whereas $K_{m(PNP)}$ and $K_{m(PCP)}$ were 3-fold lower and 2-fold higher, respectively, than $K_{m(PPi)}$. K165Q, compared with WT, displayed 20−40-fold increases in K_m for IMP and for the PPi analogues, with k_{cat} being increased by 3−4-fold (Table 3). When PNP or PCP were used by D137N, 30−75-fold reductions in k_{cat} were observed, compared to WT with the same substrates (Table 3). The kinetic mechanism of IMP pyrophosphorolysis for WT, with slow release of PRPP, results in a stimulation of Hx production in the presence of Gua as Gua traps the nascent E·PRPP complex, regenerating free enzyme through a fast guanine phosphoribosyltransfer reaction (*31*, *9*). Guanine stimulation of IMP pyrophosphorolysis was also observed with PCP (6-fold increase in the rate in the presence of Gua) and PNP (7-fold increase), indicating that PRPCP or PRPNP release is still rate-limiting in the reverse reactions using PCP or PNP as PPi analogues. No effect of guanine on the rate of IMP pyrophosphorolysis was found for K165Q with either PPi or its analogues (data not shown), suggesting that release of PRPP or PRPP analogues is no longer rate-limiting in the reverse reactions for K165Q. Gua had no effect on the rate of the IMP pyrophosphorolysis reaction catalyzed by D137N when PPi was used as the substrate. However, with PNP or PCP as the substrate, Gua (at 10 μM) caused a 2−3-fold reduction of rate of the reverse reaction. The inhibition was apparently due to the slow conversion of E·PRPNP·Gua and E·PRPCP·Gua complexes to products with D137N as noted in the preceding paragraph.

Previously, we showed that when IMP pyrophosphorolysis catalyzed by the wild-type HGPRTase was coupled to QAPRTase to remove PRPP, a 10-fold decrease of k_{cat} resulted as compared to the reverse reaction coupled to XO to remove Hx (*9*). The dependence of the rate of the reverse reaction on the nature of the coupling system indicated that product release from the E·Hx·PRPP ternary complex was random with PRPP release slower than the release of the base. K165Q also showed a 10-fold decrease in the rate of IMP pyrophosphorolysis when QAPRTase-coupled reactions were compared to XO-coupled reactions, suggesting that, as for WT, PRPP is capable of dissociating from the E·Hx·PRPP ternary complex with a rate slower than that for the base. D137N displayed a 2-fold decrease in the rate of QAPRTase-coupled IMP pyrophosphorolysis, indicating comparable rate constants for release of the base or PRPP from the E·Hx·PRPP ternary complex with D137N.

pH Dependence of K165Q and D137N. Values of k_{cat}, $k_{cat}/K_{m(PRPP)}$, and $k_{cat}/K_{m(PPi)}$ for IMP formation and pyrophosphorolysis and k_{cat} values for GMP formation catalyzed by K165Q HGPRTase were followed from pH 5.0 to 9.5. In the pyrophosphorolysis of IMP, plots of log k_{cat} versus pH for K165Q were nearly identical with those of WT with an essential acidic group with pK_a = 7.55 ± 0.08 (Figure 3A), 0.3 pH unit below that for WT. In the formation of nucleotides, log k_{cat} versus pH plots for K165Q were similar with either Hx or Gua as substrate (Figure 3B) but different from those for WT. The value of k_{cat} increased from pH 5.0 to 8.5, where it reached a plateau. The fits in Figure 3B are discussed later. Plots of log k_{cat}/K_m versus pH for PRPP were similar for K165Q and WT. One acidic (pK_a = 8.7 ± 0.3) and one basic group (pK_a = 7.7 ± 0.2) were implicated in the productive binding of PRPP to K165Q (Figure 4). As noted with WT, two basic groups and one acidic group were involved in the productive binding of PPi to K165Q (data not shown).

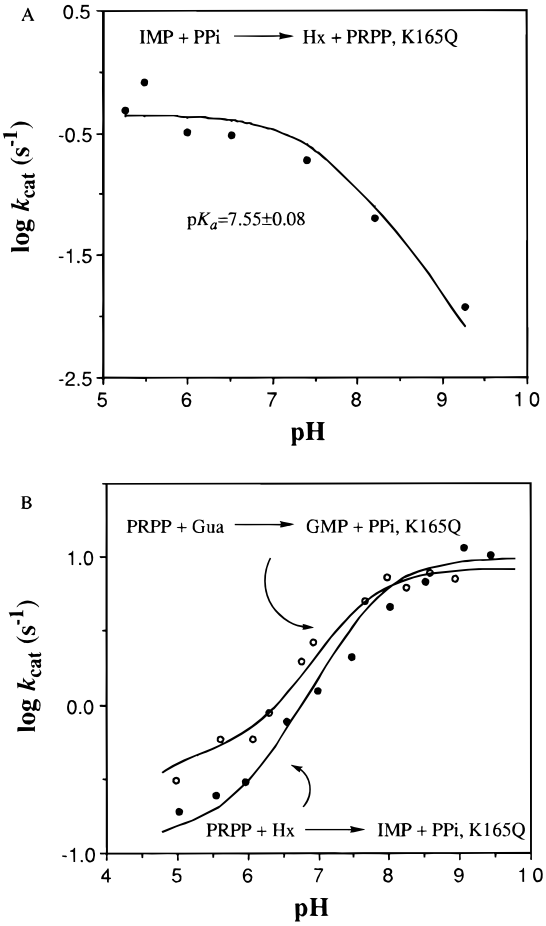

FIGURE 3: pH profiles of k_{cat} for IMP pyrophosphorolysis (A) and nucleotide formation (B) for K165Q. The line in (A) was generated using HBBELL (*23*). The lines in (B) were generated according to Scheme 3 (see Discussion) for IMP (closed circles) and GMP (open circles) formation.

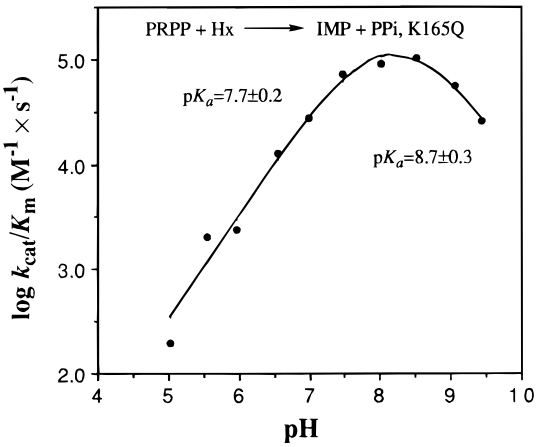

FIGURE 4: pH profile of $k_{cat}/K_{m(PRPP)}$ for K165Q. The line represents the fit using BELL (*23*).

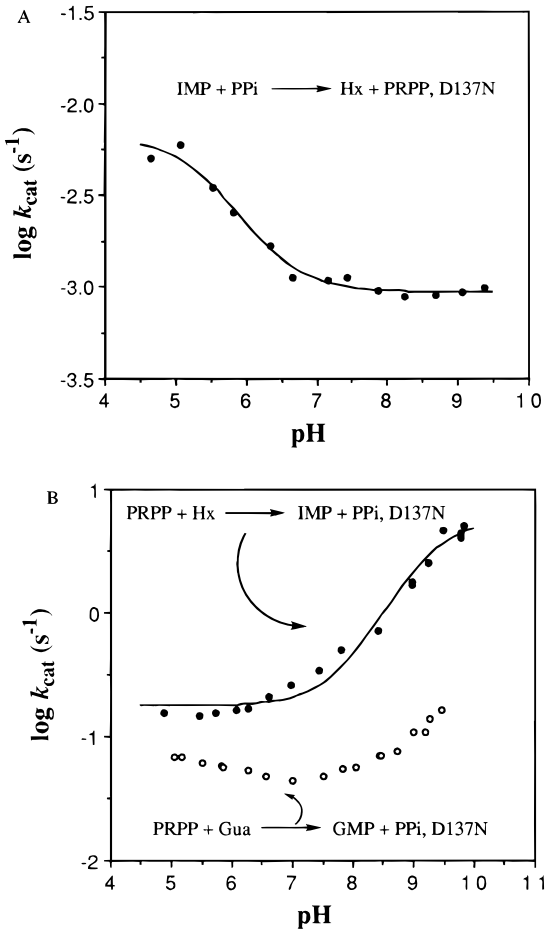

FIGURE 5: pH profiles of k_{cat} for IMP pyrophosphorolysis (A) and nucleotide formation (B) for D137N. The lines for IMP pyrophosphorolysis and IMP formation (closed circles) represent the fit using WAVL (*23*). No fit was attempted for GMP formation (open circles), and the line shown is an interpolation of the data.

Values of k_{cat} for IMP and GMP formation and IMP pyrophosphorolysis were measured for D137N from pH 4.5 to 9.5. A strikingly altered log k_{cat} versus pH plot was observed for the IMP pyrophosphorolysis reaction compared to WT (Figure 5A), with the disappearance of the essential acidic group seen with WT. For IMP formation, D137N displayed a log k_{cat} versus pH plot different from WT (Figure 5B). From pH 4.5 to 9.5, the slope of the plot gradually approached unity. For both of these reactions, the data for the low remaining activities could be fit using the WAVL program (*23*), which assumes titration between two ionization states with measurable activity. The plot of log k_{cat} versus pH for GMP formation catalyzed by D137N showed little pH dependence from pH 5.0 to 9.5 and could not be convincingly fit by HBELL or WAVL. The chemical identity and rate of formation of the nucleotide product for the slow forward reactions catalyzed by D137N at either acidic or alkaline pH ranges were verified by radiolabel transfer assays (*9*).

Ligand Interactions of K165Q and D137N. Equlibrium gel filtration was used to measure binding of PRPP to K165Q and D137N. The K_D for PRPP of K165Q was 25 μM, 20-fold increased compared to that of WT (1.2 μM; ref *9*). The K_D for PRPP of D137N was 0.32 μM, decreased by 4-fold. In both cases, binding was to a single site per subunit as for WT.

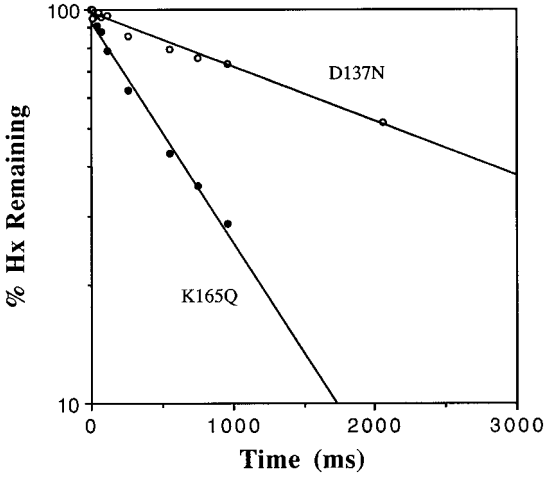

FIGURE 6: k_{on} for Hx binding to K165Q·PRPP and D137N·PRPP. E·PRPP complex was formed by incubating 4.0 μM K165Q with 1.9 mM PRPP in 100 mM Tris-HCl, 12 mM $MgCl_2$, 5 mM DTT, pH 7.4, in one syringe. The other syringe contained 0.42 μM [^{3}H]-Hx in the same buffer. For D137N, concentrations of D137N, PRPP, and [^{3}H]Hx were 4.1 μM, 1.8 mM, and 0.34 μM, respectively. Reactions were initiated when equal volumes of solution from each syringe were mixed. Reaction samples were treated as described under Materials and Methods. The lines represent the linear least-squares fit.

Nucleotide binding to the mutant enzymes was estimated by competitive displacement of [β-^{32}P]PRPP by nonlabeled nucleotide. With D137N, K_D values for GMP and IMP were found to be 4.0 and 21 μM, respectively, decreased by 2−3-fold compared to WT (7.1 and 61 μM; ref *9*). K165Q bound GMP with about 150-fold lower affinity than WT on the basis of slight inhibition of [β-^{32}P]PRPP binding observed with 1.5 mM GMP. K165Q bound IMP with at least 100-fold lower affinity since at 1.5 mM IMP no displacement of [β-^{32}P]PRPP was found (data not shown). Single-turnover experiments (*9*) were performed to determine the minimal on-rate of Hx to the E·PRPP complex for K165Q. The rate constant was determined to be 0.73×10^6 M^{-1} s^{-1} (Figure 6), somewhat higher than the steady state $k_{cat}/K_{m(Hx)}$ for this mutant enzyme (0.15×10^6 M^{-1} s^{-1}) but 26-fold reduced from the value for WT (1.9×10^7 M^{-1} s^{-1}, *9*). When similar experiments were done with D137N, the rate constant for the binding of Hx to the E·PRPP complex was determined to be 0.16×10^6 M^{-1} s^{-1} (Figure 6), 4-fold higher than the steady state $k_{cat}/K_{m(Hx)}$ for this mutant enzyme (0.04×10^6 M^{-1} s^{-1}) and 120-fold decreased compared to WT. The reduction in the rate constant for Hx binding largely accounts for the observed 19-fold increase of K_m for Hx in D137N.

Rapid Quenching Experiments with K165Q and D137N. The rate of the phosphoribosyl transfer step was assessed by performing rapid quenching experiments in the forward direction with the mutant enzymes. The pre-steady-state time course for K165Q revealed a rapid, near-stoichiometric burst of IMP formation ($k_{obs} \geq 300$ s^{-1}, about 3-fold faster than that observed with WT (*9*); $n = 1.1$ mol of IMP/mol of subunit) followed by a linear rate which represented steady-state k_{cat} (Figure 7A). A slower burst rate for GMP formation by K165Q was observed ($k_{obs} = 35$ s^{-1}, $n = 0.90$ mol of GMP/mol of subunit; Figure 7A). Given the decreased on-rate of Hx to the E·PRPP complex observed with K165Q, a slow on-rate for Gua might be expected. However, the poor solubility of Gua prevented its use in high concentrations in

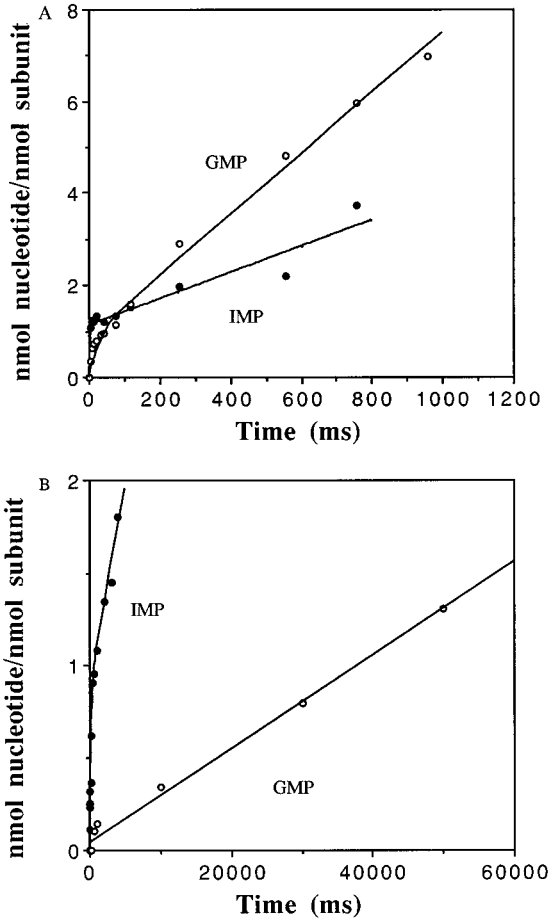

FIGURE 7: (A) Pre-steady-state formation of nucleotides (IMP, closed circles; GMP, open circles) by K165Q. One syringe contained [^{3}H]Hx or [^{14}C]Gua in 100 mM Tris-HCl, 12 mM $MgCl_2$, 5 mM DTT, pH 7.4. The other syringe contained K165Q and PRPP in the same buffer. The final concentrations of K165Q, Hx, and PRPP were 71.8 μM, 1 mM, and 2 mM, respectively, for IMP formation and 7.6 μM, 100 μM, and 1 mM, respectively, for GMP formation. The experimental procedures were the same as those in Figure 8. (B) Pre-steady-state formation of nucleotides (IMP, closed circles; GMP, open circles) by D137N. The setup of syringes was identical with that in (A). The final concentrations were 48.5 μM D137N, 500 μM Hx, and 1 mM PRPP, respectively, for IMP formation and 2.2 μM D137N, 36.8 μM Gua, and 1 mM PRPP, respectively, for GMP formation. The lines in both (A) and (B) represent the best fit to the burst kinetic equation described in Materials and Methods.

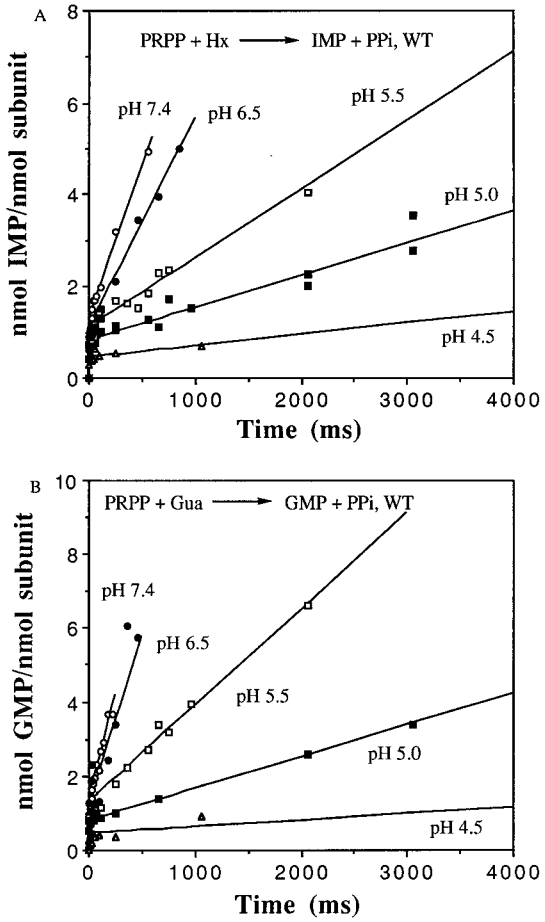

FIGURE 8: Pre-steady-state formation of IMP (A) and GMP (B) catalyzed by WT from pH 4.5 to 7.4. The setup of syringes was identical with that in Figure 7. The data sets for pH 7.4 were from Xu et al. (*9*). All the other experiments were performed in 100 mM Na-MES, 12 mM excess $MgCl_2$ over PRPP, 5 mM DTT. The final conditions for IMP formation were as follows: open circles, pH 7.4; closed circles, 1.9 mM PRPP, 94 μM Hx, 5.3 μM WT, pH 6.5; open squares, 2.0 mM PRPP, 106 μM Hx, 2.3 μM WT, pH 5.5; closed squares, the data were from two independent experiments, one with 1.6 mM PRPP, 92 μM Hx, 5.3 μM WT, pH 5.0, and the other with 5 mM PRPP, 95 μM Hx, 2.5 μM WT, pH 5.0; open triangles, 5 mM PRPP, 87 μM Hx, 5.3 μM WT, pH 4.5. The final conditions for GMP formation were as follows: open circles, pH 7.4; closed circles, 1.9 mM PRPP, 89 μM Gua, 4.2 μM WT, pH 6.5; open squares, 2.0 mM PRPP, 101 μM Gua, 2.3 μM WT, pH 5.5; closed squares, 1.6 mM PRPP, 96 μM Hx, 4.2 μM WT, pH 5.0; open triangles, 4.9 mM PRPP, 98 μM Gua, 5.3 μM WT, pH 4.5. The lines represent the best fit to the burst kinetic equation as described in the Materials and Methods.

the rapid-quench experiments, and the slower observed burst rate for GMP formation probably reflects rate-limiting binding of Gua to the E·PRPP complex.

A striking difference between Hx and Gua was observed with D137N (Figure 7B). D137N was shown to catalyze an initial burst of IMP formation (n = 1.1 mol of IMP/mol of subunit and k_{obs} = 4 s^{-1}, 33-fold decreased compared to the burst rate for WT (*9*)) followed by steady-state IMP formation. No such burst of nucleotide formation was found with Gua. Instead, GMP was formed at a linear initial rate equal to k_{cat} (0.04 s^{-1}), indicating that, unlike WT, the chemical step is rate-limiting with D137N using Gua as the substrate.

pH Dependence of Pre-Steady-State Kinetics. To better understand the steady-state kinetic pH dependence of WT HGPRTase, rapid-quenching experiments were performed at several pH values from pH 4.5 to 7.4. Both pre-steady-state IMP and GMP formation by the WT HGPRTase were followed. In these experiments, the presence of saturating amounts of PRPP at the desired pH value in the enzyme syringe allowed complexes to reach protonic equilibration with the solvent. No loss of activity was found during the course of incubation. As shown in Figure 8, the time course of nucleotide formation at all pH values was biphasic: a rapid burst followed by a slow linear phase which represented the steady-state rate. The steady-state rates from these experiments were consistent with the results from the steady-state pH dependence study. There was no appreciable change in the rate of the burst phase observed from pH 4.5 to 7.4. The burst magnitude, however, clearly varied with pH. From pH 7.4 to pH 4.5, it dropped from 1.3 mol of IMP(GMP)/mol of subunit to 0.4−0.6 mol of IMP(GMP)/

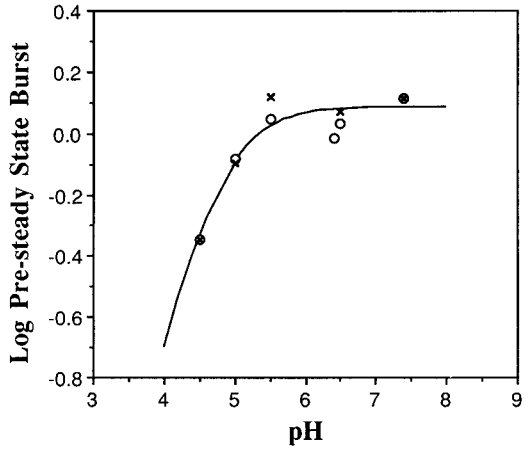

FIGURE 9: pH dependence of burst magnitude for nucleotide formation (open circles, IMP formation; crosses, GMP formation). The burst magnitudes from Figure 8 were used. The burst magnitude observed with IMP formation at pH 6.4, performed under conditions similar to those for IMP formation at pH 6.5, was also included. The line represents the fit with HABELL using the entire data set (*23*).

Scheme 2

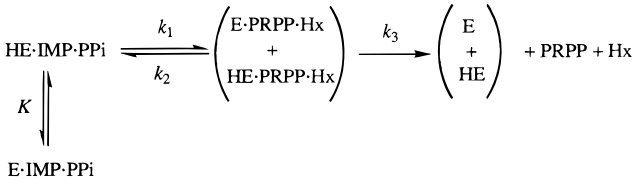

mol of subunit. Both IMP and GMP formation appeared to follow same pattern (Figure 8). A plot of the log of the burst magnitude versus pH indicated a basic group of pK_a = 4.71 ± 0.03 (Figure 9). To ensure that the lower burst magnitude was not simply due to an effect of pH on the internal equilibrium between the enzyme·base·PRPP and enzyme·nucleotide·PPi complexes, rapid-quenching experiments were performed for IMP pyrophosphorolysis at lower pH, and no compensatory increase of burst magnitude was found (data not shown).

DISCUSSION

The difference of pK_a at the N7 of the purine ring between Hx or Gua and IMP or GMP (about 11 pH units) indicates that enzymic acid/base catalysis could provide a very substantial lowering of the energetic barrier to formation and cleavage of the nucleocidic bond. The pH dependence and mutagenesis studies with HGPRTase reported here support the conclusion that the nucleotide formation and pyrophosphorolysis reactions are assisted by acid/base catalysis and demonstrate that this catalytic function is provided by Asp 137. In the reverse reaction, the pH profile of k_{cat} can be readily explained by a simple mechanism (Scheme 2) in which an essential acid at protonic equilibrium is required for catalysis. The pH dependence of the burst magnitude in the pre-steady-state formation of nucleotides confirmed that an enzymic base in its deprotonated form is necessary for the rapid conversion of the enzyme·base·PRPP complex to the enzyme·nucleotide·PPi complex, further substantiating the notion that base catalysis is integral to nucleotide formation. In the forward reaction, the pH profiles of k_{cat} for both IMP and GMP formation are consistent with the requirement for base catalysis. However, the hollows in these profiles (Figures 1B and 3B) are diagnostic of kinetic mechanisms in which protonic equilibrium is not attained (*26*). Slow proton transfer between enzymic residues and solvent has been recognized for reactions catalyzed by fumarase and aconitase (*32*, *33*).

Scheme 3, in which the rate constants for protonic equilibria can be varied, provides a good fit to the observed effects of pH on both pre-steady-state and steady-state kinetic parameters for HGPRTase, including the complex log k_{cat} versus pH plots for the forward reactions catalyzed by either WT or K165Q (Figures 1B and 3B). Scheme 3 is similar to that for catalysis at pH 7.4 presented earlier (Scheme 4; ref *9*) with the addition of enzyme/solvent equilibria (designated K_a, K_b, K_c, K_d, K_e) for an essential acid/base and the existence of two alternative pathways, with rate constants designated by k_x and k^H_x, with regard to the protonation state of the essential acid/base. In construction of Scheme 3, the rate of the chemical step for IMP and GMP formation was fixed according to the burst rate observed from pre-steady-state kinetic analysis (k_2 = 130 s^{-1} for WT and k_2 = 300 s^{-1} for K165Q). The release of nucleotide from enzyme·IMP(GMP) complexes (k_4 and k^H_4) was set to be pH-independent and rate-limiting at high pH (i.e., $k_4 = k^H_4$ = maximum k_{cat} based on pH profiles), and the rates of release of nucleobase from enzyme·Hx(Gua)·PRPP complexes (k_{-1} and k^H_{-1}) were assumed to be identical for both Hx and Gua. Finally, K_b, the protonic equilibrium constant for enzyme·Hx(Gua)·PRPP complexes, was the same for both IMP and GMP formation catalyzed by either WT or K165Q. Values for K_c and K_d (the protonic equilibria for the product complexes), and K_e (the protonic equilibrium for free enzyme) need not be specified, so long as they are assumed to be rapid. The pH-dependent rate equation (eq 3), adapted from Cleland (*26*),

$$k_{cat} = \left[\frac{k_2k_4}{k_2+k_4}\left(1+\frac{k_bk^H_{-1}\mathrm{H}}{k_{-1}(k_b+k^H_{-1})K_b}\right)\right]/ [1+[[k_2k_bk^H_{-1}+k_4(k_bk^H_{-1}+k_2k^H_{-1}+ k_{-1}k^H_{-1}+k_{-1}k_b)]\mathrm{H}/K_b+k_bk^H_{-1}k_4(\mathrm{H}/K_b)^2]/ k_{-1}(k_b+k^H_{-1})(k_2+k_4)] \quad (3)$$

was then used to calculate k_{cat} at the pH values tested, substituting various values for k_{-1}, k^H_{-1}, and k_b, k_{-b}. In Scheme 3, values for these parameters that resulted in a good fit are listed. The results were also plotted as lines in Figures 1B and 3B.

For WT utilizing Hx, the rate constant for proton transfer to solvent from HE·PRPP·Hx (k_b, 5 s^{-1}) is slow compared to the rate constants of the chemical step (k_2) and product release (k_3, k_4). With Gua, the value of k_b that yields the best fit is more comparable to k_2, k_3, and k_4. With K165Q, pH profiles were best fit when proton transfer (k_b) was even slower than with WT. The value of k_b for WT is 3 orders of magnitude slower than that expected for an acid with pK_a = 7.2 whose conjugate base undergoes diffusion-controlled association with hydronium ions (*34*). Steric hindrance by the HGPRTase protein provides a reasonable explanation for the slow proton transfer. First, N7 of the purine nucleotide is positioned directly against protein residues Asp 137 and Lys 165 and may lessen their access to solvent. Second,

Scheme 3

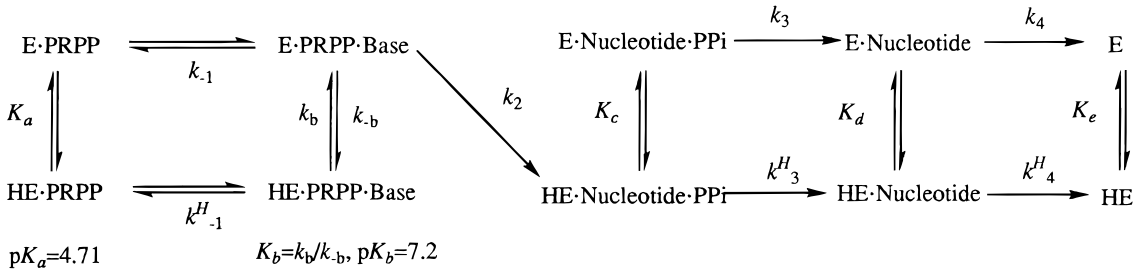

	k_{-1} (s^{-1})	k^H_{-1} (s^{-1})	k_b (s^{-1})	k_{-b} (μM^{-1} s^{-1})	k_2 (s^{-1})	$k_4=k^H_4$ (s^{-1})	k_3 & k^H_3 (s^{-1})
WT IMP	2	10	5	79	130	25	> 25
WT GMP	2	10	40	632	130	20	> 20
K165Q IMP	2	0.5	0.15	2.4	300	10	> 10
K165Q GMP	2	0.5	0.5	8	300	8.5	> 8.5

Scheme 4

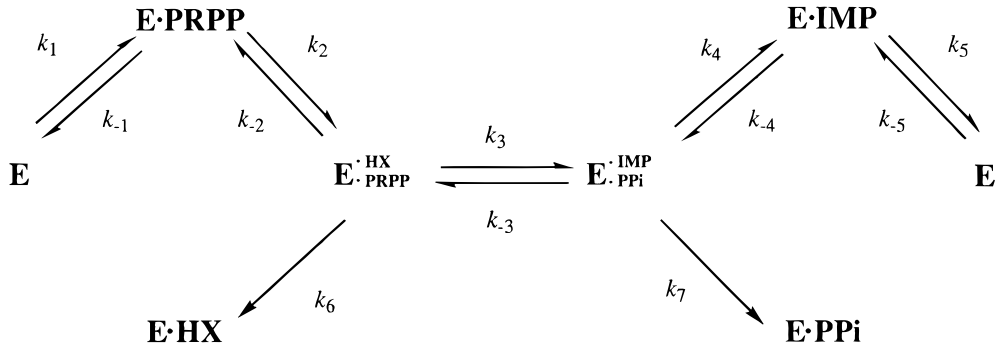

solvent occlusion of the active site during catalysis of phosphoribosyl transfer has been proposed for OPRTase (*35*, *36*) and HGPRTase (*8*, *37*). For both enzymes, a flexible loop was proposed to cover the otherwise solvent-accessible active sites to shield the oxocarbenium-like transition state (*38*) from solvolysis. Loop movement has been documented by crystal structures of OPRTase (*39*), HGPRTase (*37*), and glutamine phosphoribosylpyrophosphate amidotransferase (*40*) in which the loop was positioned directly atop the active site. It is, therefore, reasonable to postulate that the slow proton transfer to solvent might occur as a result of the steric restriction imposed by the loop movement.

Another feature of Scheme 3 is that pK_b, describing the behavior of the essential acid/base in the enzyme·PRPP·Hx ternary complex, is elevated compared to that for the PRPP bound form (7.2 vs 4.7). The pK_a indicated by the pH profile of the burst magnitude (Figure 9) represents the pK_a of the enzyme·PRPP binary complex in Scheme 3. The 3.4 kcal/mol stabilization of the protonated form of the enzymic base is unexpected, since formation of a hydrogen bond between deprotonated Asp 137 and N7 protonated Hx would be expected to lower the pK_a of the carboxyl group in these complexes. Other mechanisms to account for the increase in pK_a of Asp 137 include its proximity to the 5-phosphoryl group of PRPP, which might be closer in the catalytically active complex, or to interactions with residues in the mobile loop.

Scheme 3 can be used to describe the rates and behavior of WT at pH 7.4, the pH value used in our previous study (*9*). Scheme 3 offers good agreement with values from rapid-quench studies, in which product release was solely rate-limiting. A new feature of the current model is that in the steady state at pH 7.4 an appreciable quantity of enzyme is found in the dead-end HE·PRPP·Hx complex formed by Hx binding to HE·PRPP complex and protonation of E·PRPP·-Hx complex. Steady-state isotope trapping (*41*) could be used to test this prediction.

Following the methodology employed for WT HGPRTase (*9*), the values for individual rate constants for both mutant HGPRTases were determined (Table 4). For ease of comparison to past work, the values in Table 4 utilize Scheme 4 as the kinetic model. These rate constants reveal

Table 4: Kinetic Constants for HGPRTase[a]

constant	WT	D137N	K165Q
k_1 (M^{-1} s^{-1})	0.20×10^6	0.067×10^6	0.068×10^6
k_{-1} (s^{-1})	0.24	0.021	1.7
k_2 (M^{-1} s^{-1})	19×10^6	0.16×10^6	0.73×10^6
k_{-2} (s^{-1})	9.5	13	>8
k_3 (s^{-1})	131	4	345
k_{-3} (s^{-1})	9	0.000 39	0.19−8.6
k_4 (s^{-1})	>12	>0.32	>2.1
k_{-4} (M^{-1} s^{-1})	$>0.09 \times 10^6$	$>0.13 \times 10^6$	$>0.037 \times 10^6$
k_5 (s^{-1})	6.0	0.32	2.1
k_{-5} (M^{-1} s^{-1})	0.09×10^6	0.015×10^6	0.0019×10^6
k_6 (s^{-1})	0.28	2.5	0.7−37
k_7 (s^{-1})	12		

[a] All the rate constants refer to pH 7.4, using nomenclature outlined in Scheme 4.

that Asp 137 is the acid/base involved in catalysis. First, the pH profile of k_{cat} for D137N in the reverse reaction clearly showed the removal of the acidic group noted with WT, leading to a very dissimilar profile. The pH profiles of k_{cat} for D137N in the forward reaction were less easily interpretable. Consistent with the role for Asp 137 as the base in forward catalysis, the rates of nucleotide formation were slow for D137N. Second, the results from rapid-quench experiments revealed that the chemical step of phosphoribosyl transfer was severely impeded in D137N. The effects of mutating Asp 137 were most severe in the case of IMP pyrophosphorolysis where the rate constant for the reverse chemical step was reduced by 23 000-fold and in the case of GMP formation where a 3000-fold reduction in the rate constant for the forward chemical step was estimated. A 120-fold decrease of the rate constant for Hx binding to E·PRPP (k_2) was also observed with D137N. Third, the low activity observed with D137N was not likely due to global structural changes of the mutant enzyme since the enzyme displayed a heat stability and an aggregation state similar to those of WT, nor was it due to overall alteration of the active site since binding of substrates for D137N was actually improved.

Although D137N was severely disabled in GMP formation and pyrophosphorolysis of GMP and IMP, consistent with its role as a general acid/base, it retained a surprisingly high activity for IMP formation, suffering only a 30-fold loss in steady-state k_{cat}. In fact, the release of IMP remains rate-limiting. The pH profile of k_{cat} fit a wave function (*23*) with two poorly active forms of the enzyme, one utilizing an essential base with pK_a below 4, the other with an alternative base whose pK_a was about 9. One possible explanation for catalysis at low pH is that D137N is able to selectively stabilize a protonated IMP product at its active site, thus facilitating fast phosphoribosyl transfer only when Hx is used as the substrate. Alternatively, D137N may be able to selectively bind and stabilize the N9-deprotonated anion form of Hx, obviating a requirement of active site base. A purine anion was proposed to be the true form of the substrate for the formation of purine nucleoside catalyzed by human purine nucleoside phosphorylase (*42*). There is no known difference in the physicochemical properties between IMP and GMP, or Hx and Gua that can readily justify either hypothesis for the selective utilization of Hx. A more plausible explanation might be a selective availability of alternative modes of acid/base catalysis for IMP formation. Comparison of the crystal structures of HGPRTase complexed with either GMP or IMP (*8*, *9*) indicated that bound IMP has significantly more freedom of movement than bound GMP. Therefore, IMP (or, by analogy, Hx) might have a higher probability of attaining an exact positioning required for alternative acid/base catalysis. Substitution of water molecules for enzymic acids or bases has been proposed (*43*) and might be available to enzyme·PRPP·Hx complexes, although no ordered water molecules near N7 were revealed by the crystal structures. The ϵ-amino group of Lys 165, or a residue contributed by the flexible loop, might also be more readily accessible to bound Hx. The contribution to aicd/base catalysis provided by the 5-phosphoryl or 1-pyrophosphoryl oxygens of bound PRPP also cannot be excluded. Acid/base catalysis involving buffer ions is unlikely, since IMP formation was shown to be independent of the concentration, charge, or the identity of the buffer. Finally, it is also possible that Asn 137 itself contributes to the fast phosphoribosyl transfer chemistry observed with IMP formation catalyzed by D137N. Its unfavorable pK_a (about 15; ref *44*) makes this role unlikely. However, in thymidylate synthase, Asn 229 was suggested to contribute to acid catalysis (*43*, *45*). In the crystal structures of human and calf purine nucleoside phosphorylases, Asn 243 was found close to N7 of the bound purine substrate or analogue (*46*, *47*). Mutagenesis studies on human purine nucleoside phosphorylase (*42*, *48*, *49*) suggested that Asn 243 plays a far more important role in assisting in the phosphorolysis of the inosine nucleosidic bond than in its formation.

The data unequivocally rule out Lys 165 as an essential residue for catalysis but are consistent with a role in base binding. The K165Q mutant HGPRTase, like WT, was capable of catalyzing rapid phosphoribosyl transfer chemistry in rapid-quench experiments. The effects of pH on steady-state kinetic parameters (Figure 3) can be rationalized with Scheme 3 as for WT with individual rate constants modified. In particular, the plot of log of k_{cat} versus pH for K165Q-catalyzed IMP pyrophosphorolysis was almost superimposable with that for WT, indicating that Lys 165 is not essential and does not perturb the pH titration behavior of Asp 137. Nonetheless, Lys 165 does play an important role in binding substrates as evidenced by increased K_m and K_D values for K165Q. The increases were mainly caused by slower rate of association of Hx to the E·PRPP complex (26-fold reduction of k_2) and of IMP to the apoenzyme (47-fold reduction of k_{-5}; see Table 4 and Scheme 4). The weak binding of bases and nucleotides to K165Q is explainable by the loss of a hydrogen bond between the ϵN of Lys 165 and O6 of the purine ring seen in the crystal structure of HGPRTase complexed with GMP and IMP (*8*, *9*). The rate of release of PRPP from E·PRPP was increased by 7-fold and is no longer rate-limiting in the reverse reaction, a prediction validated by the fact that Gua had no effect on IMP pyrophosphorolysis catalyzed by K165Q.

ACKNOWLEDGMENT

We thank Dr. Vern Schramm for helpful comments on the manuscript.

REFERENCES

1. Seegmiller, J. E., Rosenbloom, F. M., and Kelley, W. N. (1967) *Science 155*, 1682−1684.
2. Lesch, M., and Nyhan, W. L. (1964) *Am. J. Med. 36*, 561−570.
3. Stout, J. T., and Caskey, C. T. (1989) in *The Metabolic Basis of Inherited Disease* (Scriver, C. R., Beaudet, A. L., Sly, W. S., and Valle, D., Eds.) pp 1007−1028, McGraw-Hill, New York.
4. Kelley, W. N., Rosenbloom, F. M., Henderson, J. F., and Seegmiller, J. E. (1967) *Proc. Natl. Acad. Sci. U.S.A. 57*, 1735−1739.
5. Senft, A. W., and Crabtree, A. (1983) *Pharmacol. Ther. 20*, 341−356.
6. Dovey, H. F., McKerrow, J. H., and Wang, C. C. (1984) *Mol. Biochem. Parasitol. 11*, 157−168.
7. Ullman, B., and Carter, D. (1995) *Infect. Agents Dis. 4*, 29−40.
8. Eads, J. C., Scapin, G., Xu, Y., Grubmeyer, C., and Sacchettini, J. C. (1994) *Cell 78*, 325−334.

9. Xu, Y., Eads, J. C., Sacchettini, J. C., and Grubmeyer, C. (1997) *Biochemistry 36*, 3700−3712.
10. Dunn, D. B., and Hall, R. H. (1975) in *Handbook of Biochemistry and Molecular Biology*. *Nucleic Acids*, 3rd ed. (Fasman, G. D., Ed.) Chemical Rubber Co., Cleveland, OH, pp 65−215, Vol. I.
11. Lister, J. H. (1979) in *Advances in Heterocyclic Chemistry* (Katrizky, A. R., and Boulton, A. J., Eds.) Academic Press, New York, *Vol. 24*, pp 215−246.
12. Zoltewicz, J. A., Clark, D. F., Sharpless, T. W., and Grahe, G. (1970) *J. Am. Chem. Soc. 92*, 1741−1750.
13. Garrett, E. R., and Mehta, P. J. (1972) *J. Am. Chem. Soc. 94*, 8532−8541.
14. Horenstein, B. A., Parkin, D. W., Estupinan, B., and Schramm, V. L. (1991) *Biochemistry 30*, 10788−10799.
15. Gopaul, D. N., Meyer, S. L., Degano, M., Sacchettini, J. C., and Schramm, V. L. (1996) *Biochemistry 35*, 5963−5970.
16. Degano, M., Gopaul, D. N., Scapin, G., Schramm, V. L., and Sacchettini, J. C. (1996) *Biochemistry 35*, 5971−5981.
17. Mentch, F., Parkin, D. W., and Schramm, V. L. (1987) *Biochemistry 26*, 921−930.
18. Kline, P. C., and Schramm, V. L. (1993) *Biochemistry 32*, 13212−13219.
19. Ho, S. N., Hunt, H. D., Horton, R. M., Pullen, J. K., and Pease, L. R. (1989) *Gene 77*, 51−59.
20. Brennand, J., Konecki, D. S., and Caskey, C. T. (1983) *J. Biol. Chem*, *258*, 9593−9596.
21. Kopetzki, E., Schumacher, G., and Buckel, P. (1989) *Mol. Gen. Genet 216*, 149−155.
22. Jolly, D. J., Okayama, H., Berg, P., Esty, A. C., Filpula, D., Bohlen, P., Johnson, G. G., Shively, J. E., Hunkapillar, T., and Friedmann, T. (1983) *Proc. Natl. Acad. Sci. U.S.A. 80*, 477−481.
23. Cleland, W. W. (1979) *Methods Enzymol. 63*, 103−139.
24. Johnson, K. (1995) *Methods Enzymol. 249*, 38−61.
25. Segel, I. H. (1975) *Enzyme Kinetics*, Wiley: New York, pp 813−818.
26. Cleland, W. W. (1977) *Adv. Enzymol. 45*, 273−387.
27. Holden, J. A., and Kelley, W. N. (1978) *J. Biol. Chem. 253*, 4459−4463.
28. McClard, R. W., Fischer, A. C., Mauldin, S. K., and Jones, M. E. (1984) *Bioorg. Chem. 12*, 339−348.
29. Ozturk, D. H., Dorfman, R. H., Scapin, G., Sacchettini, J. C., and Grubmeyer, C. (1995) *Biochemistry 34*, 10755−10763.
30. Plapp, B. V. (1995) *Methods Enzymol. 249*, 91−119.
31. Salerno, C., and Giacomello, A. (1979) *J. Biol. Chem. 254*, 10232−10236.
32. Walsh, C. (1979) *Enzymatic Reaction Mechanisms*, W. H. Freeman and Co., San Francisco, pp 525−535.
33. Rose, I. A., Warms, J. V. B., and Yuan, R. G. (1993) *Biochemistry 32*, 8504−8511.
34. Fersht, A. (1985) *Enzyme Structure and Mechanism*, Freeman, New York.
35. Scapin, G., Grubmeyer, C., and Sacchettini, J. C. (1994) *Biochemistry 33*, 1287−1294.
36. Scapin, G., Ozturk, D. H., Grubmeyer, C., and Sacchettini, J. C. (1995) *Biochemistry 34*, 10744−10754.
37. Schumacher, M. A., Carter, D., Roos, D. S., Ullman, B., and Brennan, R. G. (1996) *Nature Struct. Biol.* 3, 881−887.
38. Tao, W., Grubmeyer, C., and Blanchard, J. S. (1996) *Biochemistry 35*, 14−21.
39. Henriksen, A., Aghajari, N., Jensen, K. F., and Gajhede, M. (1996) *Biochemistry 35*, 3803−3809.
40. Krahn, J. M., Kim, J. H., Burns, M. R., Parry, R. J., Zalkin, H., and Smith, J. L. (1997) *Biochemistry 36*, 11061−11068.
41. Wilkinson, K. D., and Rose, I. A. (1979) *J. Biol. Chem. 254*, 12567−12572.
42. Erion, M. D., Stoeckler, J. D., Guida, W. C., Walter, R. L., and Ealick, S. E. (1997) *Biochemistry 36*, 11735−11748.
43. Liu, L., and Santi, D. V. (1993) *Proc. Natl. Acad. Sci. U.S.A. 90*, 8604−8608.
44. Streitwieser, A., Jr., and Heathcock, C. H. (1976) *Introduction to Organic Chemistry*, Macmillan Publishing, New York, p 494.
45. Huang, W., and Santi, D. V. (1997) *Biochemistry 36*, 1869−1873.
46. Ealick, S. E., Babu, Y. S., Bugg, C. E., Erion, M. D., Guida, W. C., Montgomery, J. A., and Secrist, J. A., III (1991) *Proc. Natl. Acad. Sci. U.S.A.* 88, 11540−11544.
47. Koellner, G., Luic, M., Shugar, D., Saenger, W., and Bzowska, A. (1997) *J. Mol. Biol. 265*, 202−216.
48. Erion, M. D., Takabayashi, K., Smith, H. B., Kessi, J., Wagner, S., Höhger, S., Shames, S. L., and Ealick, S. E. (1997) *Biochemistry 36*, 11725−11734.
49. Stoeckler, J. D., Poirot, A. F., Smith, R. M., Parks, R. E., Jr., Ealick, S. E., Takabayashi, K., and Erion, M. D. (1997) *Biochemistry 36*, 11749−11756.

BI972519M